

Supplementary Figures:
Shear-banding in surfactant wormlike micelles
Elastic instabilities and wall slip

M.A. Fardin,^{1,2} T. Divoux,³ M.A. Guedeau-Boudeville,¹ I. Buchet-Maulien,⁴
J. Browaeys,¹ G.H. McKinley,² S. Manneville,^{3,5} and S. Lerouge^{1,*}

¹*Laboratoire Matière et Systèmes Complexes, CNRS UMR 7057*

Université Paris Diderot, 10 rue Alice Domont et Léonie Duquet, 75205 Paris Cédex 13, France

²*Department of Mechanical Engineering*

Massachusetts Institute of Technology, 77 Massachusetts Avenue, MA 02139-4307 Cambridge, USA

³*Université de Lyon, Laboratoire de Physique, CNRS UMR 5672*

Ecole Normale Supérieure de Lyon, 46 Allée d'Italie, 69364 Lyon cedex 07, France

⁴*Laboratoire Itodys, CNRS UMR 7086*

Université Paris Diderot, 15 rue Jean de Baïf, 75205 Paris Cédex 13, France

⁵*Institut Universitaire de France*

(Dated: November 24, 2011)

* Corresponding author ; sandra.lerouge@univ-paris-diderot.fr

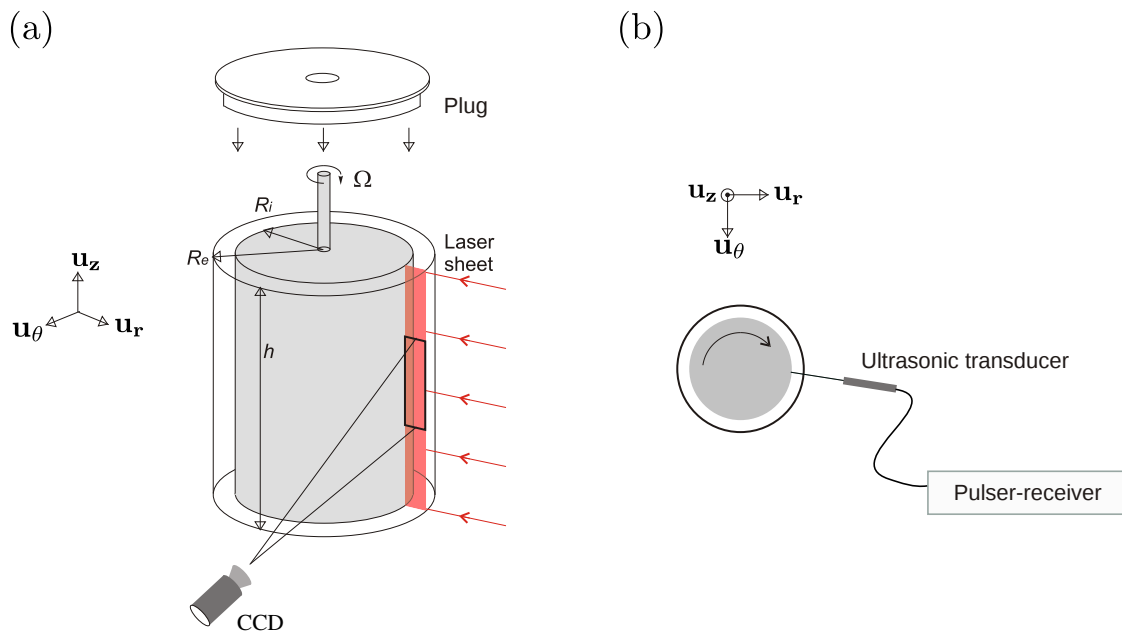


FIG. 1. (a) The experimental setup for the observation of the gap in the plane (r, z) . (b) Top view of the Couette cell and of the measurement configuration for ultrasonic velocimetry. In both cases, the outer cylinder is surrounded by water which keeps the sample at a constant temperature.

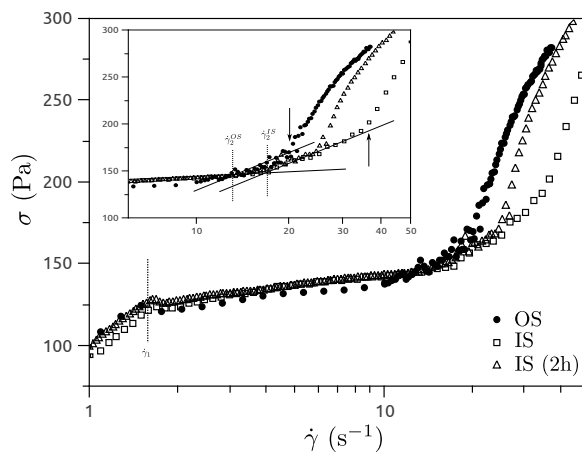


FIG. 2. Stress plateau and dynamical upper branch for the OS (\bullet), IS (\square) and a sample irradiated for 2 hours (\triangle). Inset: Enlargement of the transition region between the stress plateau and the apparent high shear rate branch. The arrows delimit the turbulent bursts regime from the fully turbulent state.

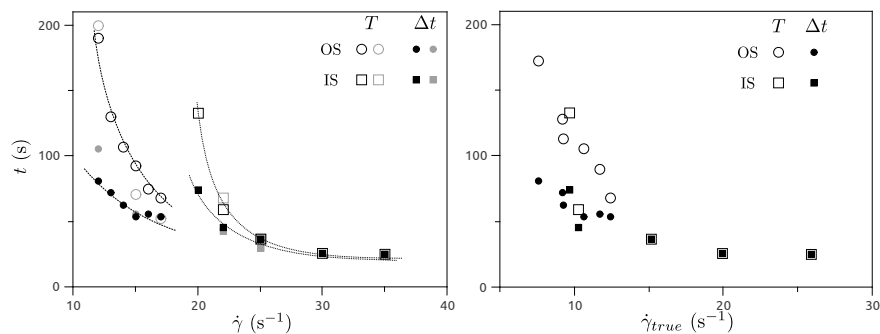


FIG. 3. Characteristic times related to the development of turbulent bursts for the OS (circles) and IS (squares) at a given position along the vorticity direction, as a function of (a) $\dot{\gamma}$ and (b) $\dot{\gamma}_{true}$. T (open symbols) represents the mean temporal period between successive bursts while Δt (close symbols) represents their live time. Black and light grey symbols distinguish between data respectively extracted from USV and optical experiments. Continuous lines are guides for the eyes.

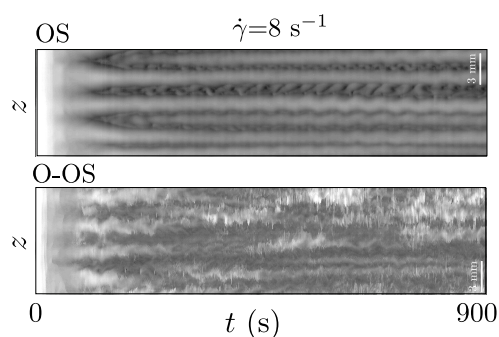


FIG. 4. Comparison of the spatiotemporal diagrams of the interface position at $\dot{\gamma}=8 \text{ s}^{-1}$ for the OS and O-OS. The dynamics of the O-OS are essentially similar to the dynamics of the IS.

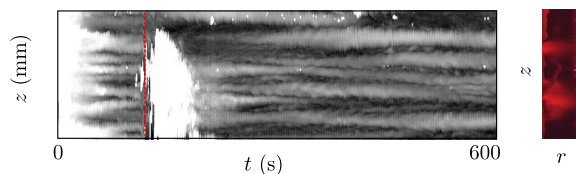


FIG. 5. Spatiotemporal diagram of the interfacial position at $\dot{\gamma}=20 \text{ s}^{-1}$ for the IS. The white patch corresponds to the nucleation and growth of a turbulent burst away from the edges of the Taylor-Couette cell. The picture on the right-hand side is the snapshot of the (r, z) plane associated with the red line in the diagram.

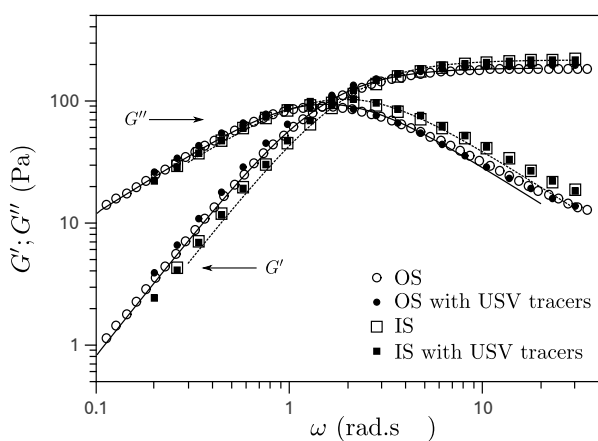


FIG. 6. Storage modulus G' and loss modulus G'' as a function of the angular frequency ω for the OS and IS with (closed symbols) and without (open symbols) USV tracers. In each case, a 5% sinusoidal deformation has been applied over a frequency range from 0.1 to 30 rad/s. The continuous and dotted lines correspond to the best fits computed from the Maxwell model for the OS and IS respectively. The results are summarized in Table I of the paper.

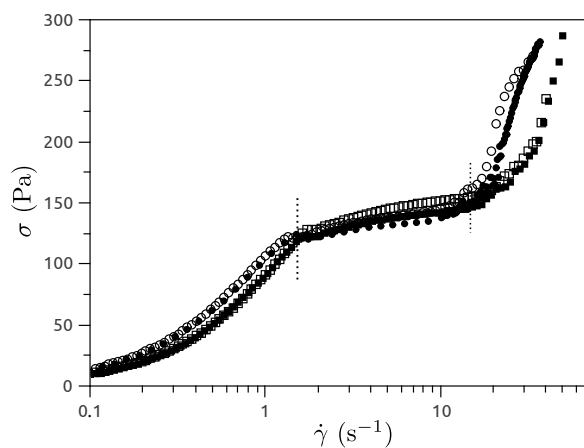


FIG. 7. Semi-logarithmic plot of the steady state flow curves of the OS (open circles) and IS (open squares) measured under strain-controlled conditions. The sampling of the shear rate sweep is 120 s per data point. For comparison, the flow curves of the same samples seeded with USV tracers are given in closed symbols. The dotted lines approximately indicate the apparent limits of the stress plateau.

Electronic Supplementary Information: More details on the photochemistry of CPCI-NaSal solutions

M.A. Fardin,^{1,2} M.A. Guedeau-Boudeville,¹ I. Buchet-Maulien,³ and S. Lerouge^{1,*}

¹Laboratoire Matière et Systèmes Complexes, CNRS UMR 7057

Université Paris Diderot, 10 rue Alice Domont et Léonie Duquet, 75205 Paris Cédex 13, France

²Department of Mechanical Engineering

Massachusetts Institute of Technology, 77 Massachusetts Avenue, MA 02139-4307 Cambridge, USA

³Laboratoire Itodys, CNRS UMR 7086

Université Paris Diderot, 15 rue Jean de Baïf, 75205 Paris Cédex 13, France

(Dated: November 25, 2011)

In this ESI, we study the photochemistry of cetylpyridinium chloride solutions. We show that the cetylpyridinium chloride surfactant molecules exhibit a photochemistry mainly influenced by the photo-induced cleavage of the pyridine ring. Using UV-visible spectroscopy and nuclear magnetic resonance spectroscopy, we show that UV radiation close to the absorption band of the pyridine produces a cleavage of the ring. The reaction is irreversible, in contrast to the photoreaction of pure pyridine in neutral water, but similarly to photo-reactions of pyridine in polymeric environment. The cleavage of the ring yields an unstable aldehyde enamine, which further decays by thermally activated processes. The final products seem to include the free fatty hexadecane tails of the original surfactant, which are not miscible with the original solution, and which possibly build up a lubrication layer responsible for the anomalous flow dynamics exposed in the article.

INTRODUCTION

In the article, we have shown that the shear-banding flow of cetylpyridinium chloride solutions (CPCI) with sodium salicylate (NaSal) as a co-surfactant [1] could exhibit two classes of behaviours. Original samples behaved according to the ‘regular’ shear-banding scenario with secondary flows triggered by elastic instabilities, while ‘aged’ samples behaved abnormally, the characteristics of the base flow and of the secondary flows being perturbed, partly due to an enhanced wall slip at the boundary in contact with the high shear rate band. We realized that samples could be aged rapidly by exposing them to UV radiations, and we postulated that some photochemical reaction was creating impurities responsible for the enhanced wall slip. Here, we study in details the effect of light on cetylpyridinium chloride solutions to confirm the production of impurities by the photo-induced cleavage of the pyridine ring.

The interplay between photochemistry and rheology is a problem that has been investigated at least since a study by Müller *et al.* in 1984 [2]. They studied solutions of cetyl-trimethylammonium bromide (CTAB) with the addition of anthracenes. The latter photodimerization of the anthracenes could then trigger substantial modifications of the linear rheology [2]. A few years later, they coined the term “photorheological fluids” [3]. Recently, the interest for those “photorheological fluids” has been revived, because of their potential applications as material with quickly tunable mechanical properties [4–6], in a way similar to magneto- or electro-

rheological fluids [7]. A review on the self-assembly of light-sensitive surfactants even made the cover of the fifth issue of Soft Matter [8]. But in all of the photorheological fluids discussed so far, drastic modifications of the linear rheology have been reported, and indeed, surfactants were engineered toward this end. In the case we describe here, the situation is more subtle, since it is the flow dynamics in the non-linear regime that are affected more than the mechanical properties of the material. In fact, we have seen in the article that the linear rheology of original and aged samples was very similar and that the difference of behaviour could only be noticed by a careful observation of the flow kinetics at high shear rates, in the shear-banding regime. We have seen in the article that the differences in behaviour were linked to an enhanced wall slip, and we postulated this enhanced slip to be due to a lubrication layer at the moving wall. Our hypothesis is that light exposure of the CPCI solutions produces a small amount of immiscible product, which then enhances wall slip. As noticed in the article, the aged solutions are usually slightly yellow, a detail not necessarily highlighted in publications, but noticed by many researchers. Our hypothesis would then suggest that the immiscible product of the photochemical reaction is also responsible for the slight colouration of the aged samples.

CPCI is a surfactant whose hydrophilic head is essentially formed by a pyridine ring, C₅H₅N. And it is known that the pyridine molecule is particularly sensitive to light. In aqueous solution, the pyridine ring can be opened by UV radiation, close to the pyridine absorption band at 253.7nm [9, 10]. Photohydration of pyridine cleaves the pyridine ring and produces aldehyde enamine (5-amino-2,4-pentadienal) with other intermediate steps involving thermally unstable products like a Dewar pyri-

* Corresponding author ; sandra.lerouge@univ-paris-diderot.fr

dine [9, 10]. If the sample is protected from light and the solution pH neutral, the reaction was found to be reversible, with a half time of 2.5 min at 25°C [9, 10]. More recently, Vaganova *et al.* showed that the photo-induced cleavage-closure of pyridine could also happen in very viscous polymer solutions [11]. In this case, the kinetics of the reaction were shifted to much larger time scales, and the product of the pyridine cleavage could be stored in the material over a month, changing significantly the electronic and optical properties of the polymeric sample [11].

It then seems reasonable to expect that even as part of the CPCl surfactant, the pyridine ring will still undergo photo-induced cleavage. Moreover, the fatty chain of the pyridinium may prevent the reversibility of the reaction, in a way similar than for polymer solutions [11]. Nonetheless, photochemical reactions in micellar solutions can have unexpected outcomes [12], thus motivating a thorough study of the reaction in conditions corresponding to the one present in our rheological experiments.

In section I, we detail the composition of our samples and the spectroscopic techniques used in our study. In section II A 1, we show that the co-surfactant NaSal and the small quantity of added brine are not essential to the photoreaction. Subsequently, we work with pure CPCl solutions. We also describe preliminary kinetics of the photoreaction, helping to identify the adequate solution concentrations for the various spectroscopic protocols. In sections II B, we expose in details the results from UV-visible spectroscopy, and in section II C, the results from nuclear magnetic resonance. In section III, we discuss our result and we propose a scenario for the photodegradation of CPCl, and how it can lead to lubrication layers. Finally, we conclude in section IV.

I. EXPERIMENTAL DETAILS

A. Samples

In the article, rheology was conducted on samples made of 8.09 wt.% (0.238 M) CPCl with 1.91 % (0.119 M) NaSal in water with 0.5 M sodium chloride (NaCl). In the rheology literature, this solution is usually called CPCl 10 % for the sum of the surfactant (CPCl) and co-surfactant (NaSal) weight fractions [1, 13]. The CPCl and NaCl were purchased from Sigma-Aldrich and the NaSal from Acros-Organics. The CPCl is in a monohydrated form. A cautious sample preparation should therefore take into account the water molecule to compute the weight fraction.

In the article, we distinguished two kinds of samples, ‘the original’ sample (OS), prepared as described above, and an ‘irradiated’ sample (IS) that had the same preparation protocol with the addition of an irradiation exposure to UV light at 254 nm, the absorption band of pyridine [9]. Except if mentioned otherwise, the samples used are aqueous solutions of pure CPCl. We mainly study two

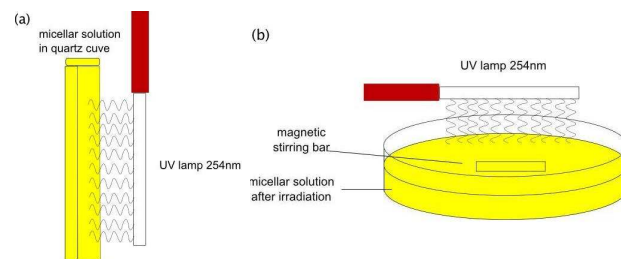


FIG. 1. Scheme of the two different irradiation set-ups. (a) Protocol 1. (b) Protocol 2.

concentrations, a 10 wt.% CPCl (0.3M), and a 0.05 wt.% (1.4 mM) solution, which corresponds to a concentration just above the critical micelle concentration (information from provider). As in the article, we distinguish irradiated and non-irradiated samples by the IS and OS abbreviations.

To irradiate the samples, we used two protocols depicted in Fig 1. Qualitative experiments were done by irradiating the micellar medium directly in a quartz UV-Visible cell, with a thickness of 2 mm, on 1 mL of surfactant solution. The UV irradiation was made with a mercury vapour pen ray lamp, with wavelength of 254 nm (UVP, USA), the lamp was put vertically at approximately 1 mm of the quartz cuve. We call this protocol, ‘protocol 1’. Quantitative experiments were done by irradiating a 30 mL surfactant solution laid out in a crystalliser, with the same UV pen ray lamp, 254 nm, placed horizontally at approximately 1-2 cm of the solution stirred by a magnetic bar. We call this protocol, ‘protocol 2’. In both protocols, we homogenize and increase the irradiation by covering the set-up with aluminium foil, brilliant face turned towards the interior. The irradiation was done at room temperature for protocol 1 and at 40°C for protocol 2.

In any cases, when not used, and if not otherwise stated, the samples were stored at room temperature and protected from light exposure by covering containers with aluminium foil. In what follows, we use t_{ir} to stand for the duration of irradiation by UV light, and we call t_a the time during which samples were stored prior to a given experiment—not only rheological, but also spectroscopic.

B. Techniques

In order to identify changes in the chemical compositions of solutions of CPCl after light exposure, we use two different spectroscopic techniques.

We used UV-visible spectroscopy, for wavelengths λ between 200 nm and 600 nm and we measure the optical density (OD) of the absorption bands.

We also performed proton NMR (^1H NMR). The proton spectra were carried out with a NMR Bruker, 500 MHz. Integrations were made by giving the value of 3

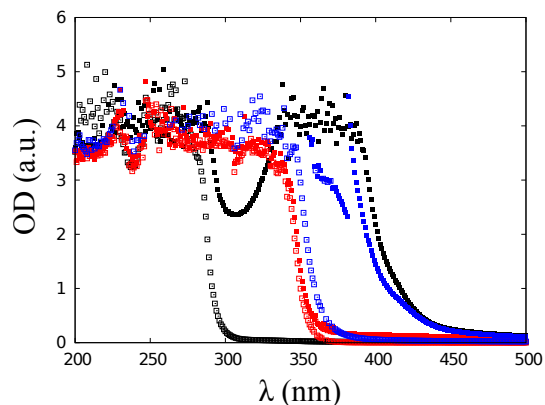


FIG. 2. Preliminary UV-visible spectra of OS (open symbols) and IS (filled symbols). In blue, semi-dilute samples used in rheological experiments in I. (with NaSal and NaCl). In red, 2wt.% NaSal solutions. In black, 10wt.% CPCl solutions. For irradiated solutions, we have $t_{ir} = 30\text{min}$ and $t_a \simeq 1 - 3\text{h}$.

to the three protons of the group methyl. Therefore, for each peak, whatever the chemical shift, each proton has a value of 1. NMR was done on 0.05 wt.% samples. The samples were irradiated with protocol 2. We then measured their UV-visible spectra before the solutions were freeze-dried. The powders thus obtained, roughly 15 mg for each irradiation duration, were then dissolved in CDCl_3 , 0.5 mL to 0.7 mL depending on the solubility of the new products, in order to have a concentration high enough (2.15% to 3%) to carry out the ^1H NMR experiments to see the evolution of the molecular structure as a function of the duration of irradiation t_{ir} . In the discussion section, we also show micrographs taken from an optical light microscope. In this case, we used a hermetic cell composed, from down to up, of a glass cover slip, a spacer of 1 mm, the original CPCl 10% micellar solution with salts, used in rheological experiments and, at the top, a quartz slide, the whole being inserted in a metal support, closed using screw. The top quartz surface could then allow irradiation with a protocol essentially similar to protocol 1. The cell was then posed on a turntable of an inverted microscope, and micrographs were taken with 10X, 20X and 60X objectives.

II. RESULTS

A. Preliminary observations

1. Irrelevance of salts

In order to assess the strength of our hypothesis, we first performed a few qualitative experiments on the rheological CPCl samples, with NaSal co-surfactant and 0.5 M NaCl. We had noted a shift in color for the IS

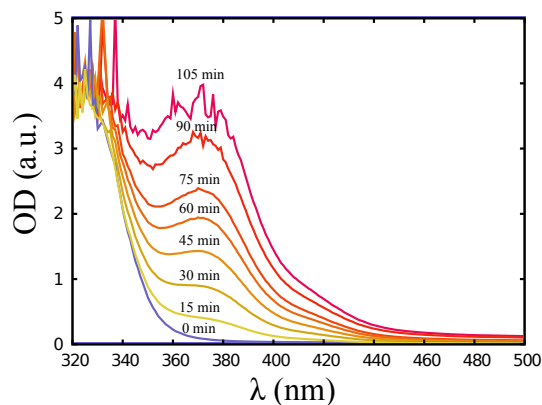


FIG. 3. UV-visible spectra of CPCl samples at 10wt.% irradiated using protocol 2, for $t_{ir} = 0, 15, 30, 45, 60, 75, 90$ and 105 min. All the spectra were measured right after irradiation ($t_a \simeq 0$).

that we wished to quantify by spectroscopy. We wanted to see if salts had any bearing on the photochemistry. In those experiments, irradiation was done using protocol 1 with $t_{ir} = 30$ min and t_a on the order of a few hours. Fig. 2 shows typical spectra for the IS and OS of various compositions. On the OS of the micellar solution with salts used in the article, the OD sharply increases around 360 nm and then saturates. Whereas on the IS, the spectrum shifts to higher wavelengths and saturates around 400 nm. In contrast, solutions of pure NaSal show only a weak change of the spectrum before and after UV irradiation, with in both cases, a sharp increase of OD around 360 nm, where the OS of the micellar solution with salts saturated. The pure 10wt.% CPCl sample, without any salt, shows a sharp increase of OD around 300nm for the OS, whereas on the IS, the spectrum shifts to higher wavelengths and saturates around 400nm, in a way similar to the IS of the micellar solution with salts. From Fig. 2, it is manifest that UV radiations have almost no impact on NaSal. Thus, we can conclude that it is the molecule of CPCl which is implicated in the problem of ageing of the micellar solutions, and in what follows, we will only use solutions of pure CPCl. Note also, that during this preliminary phase, we did not observe a visible difference on the irradiation effects between solutions made with pure water purged with nitrogen or oxygen. Thus, the free radicals causing this bathochrome effect on the absorption band do not come simply from the oxygen dissolved in the solution. This fact was indeed noticed previously in the case of pure pyridine [10]. Therefore, in what follows, we did not take any further precautions regarding the quantity of dissolved oxygen in our samples.

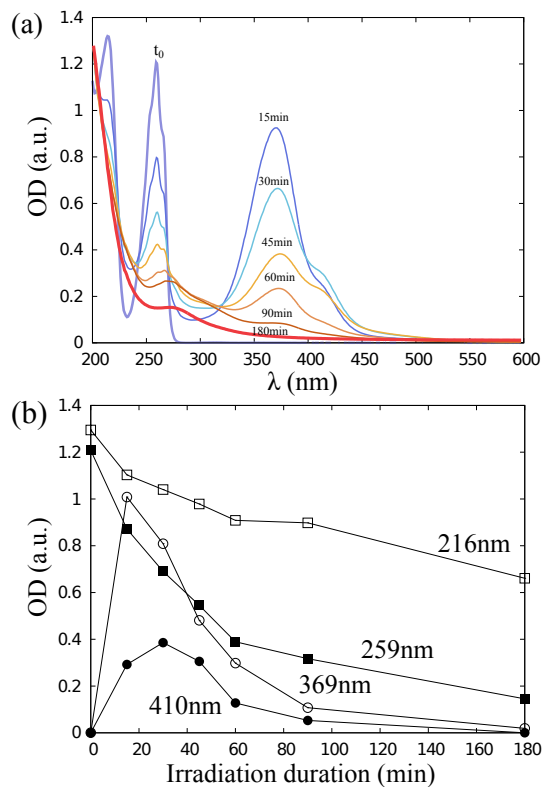


FIG. 4. Photochemical kinetics for various irradiation durations. (a) UV-visible spectra of 0.05wt.% CPCl solutions for $t_{ir} = 0, 15, 30, 45, 60, 90$ and 180 min. (b) Optical density (OD) as a function of the irradiation duration for four wavelength 216 nm, 259 nm, 369 nm and 410 nm.

2. Preliminary kinetics

In the previous experiments, we had quite arbitrarily limited the irradiation time to $t_{ir} = 30$ min. On Fig. 3 we show the unsaturated part of four spectra taken just after UV radiation for t_{ir} ranging between 15 min and 105 min. We can observe the emergence of a new absorption band around 360 nm, growing with the irradiation duration. It confirms that a photochemical reaction is taking place. But the concentrations used were too high to resolve full spectra, because of saturation effects. The saturation was already manifest on Fig. 2.

In order to find a suitable concentration to avoid saturation effects in spectroscopy, we made a few solutions of decreasing concentration of pure CPCl, from the original 10 wt.% solution to the suitable 0.05 wt.% dilute solution.

B. Kinetics study using UV-visible spectroscopy

1. Kinetics on dilute samples under UV-irradiation

For solutions of CPCl at 0.05 wt.% the changes in absorption can be measured fully on the UV-visible spectra. The spectrum of the solution without any irradiation is given on Fig. 4(a), as the curve labelled by ' t_0 '. The sharp peak at 254 nm corresponds to the absorption band of the pyridine ring [9]. With protocol 2, we then irradiated the CPCl solutions at 0.05wt.% to see the evolution of the maximum of absorption band. Fig. 4(a) shows spectra measured for various t_{ir} between 15 min and 180 min. Further irradiation beyond 180 min did not modify the spectrum significantly. As for the concentrated solution, we can observe the creation of a new absorption band around 360nm, more precisely identified as 369 nm, with a shoulder at 410 nm, corresponding to the absorption of a new molecule. Since the OD does not saturate, we can also observe the progressive disappearance of the band at 254 nm, corresponding to the absorption of the pyridine ring.

A substantial difference with the preliminary kinetics realized in concentrated solutions, is that the emergence of the new absorption band happens much quicker in the dilute solution. After 15 min of irradiation, the maximum absorption at 369 nm has already been reached and further irradiation seems to only trigger the disappearance of this transient peak.

To summarize the photochemical events, in Fig. 4(b) we show the evolution of the optical density with the duration of irradiation for four characteristic wavelengths. At 216 nm and 259 nm, the optical density decreases continuously with the time of irradiation t_{ir} , corresponding to the disappearance of pyridine. Whereas at 369 nm and 410 nm, bands not existing before quickly appear and then disappear with further increase of the irradiation time. Note that on more concentrated solutions discussed previously, the OD of the band at 369 nm was still increasing after $t_{ir} = 300$ min. It is then manifest that the radiation efficiency in dilute solutions is much higher than in the concentrated solutions, which quickly cut off the UV light, necessary to generate the creation of the transient species.

We also studied the effect of the wavelength on the appearance of the transient species. The emergence of the absorption band at 369 nm could also be triggered by UV light at 365 nm, but at a rate three time lower (data not shown).

2. Kinetics on dilute samples after UV-irradiation

Since the maximum of absorption on 0.05 wt.% CPCl solutions had been reached already after $t_{ir} = 15$ min, we only irradiated the solution for $t_{ir} = 15$ min with protocol 1, and we then stored the sample in the dark at room temperature, and measured spectra for various

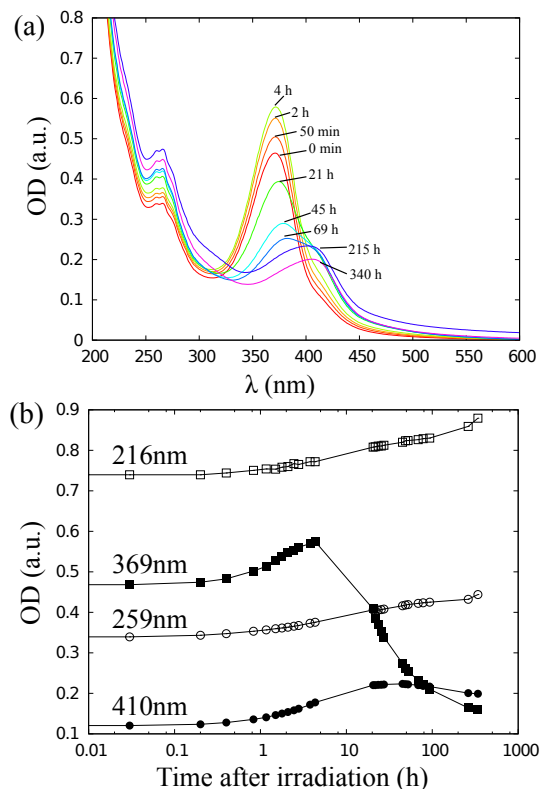


FIG. 5. Photochemical kinetics of 0.05 wt.% CPCl solutions for various time after irradiation for $t_{ir} = 15$ min. (a) UV-visible spectra for $t_a = 0, 50$ min, 2 h, 4 h, 21 h, 45 h, 69 h, 215 h and 340 h. (b) Optical density as a function of t_a for four maxima of wavelength 216 nm, 259 nm, 369 nm and 410 nm.

time after irradiation ranging from a few minutes to two weeks. Fig. 5(a) shows the evolution of the spectra for various values of t_a . For $t_a = 0$, *i.e.* just after the 15 min of irradiation, the absorption band of the pyridine, at 254 nm, has been significantly reduced, and a new absorption band has appeared around 369 nm. From $t_a = 0$ to $t_a \simeq 4$ h, the optical density of this new band keeps increasing. Eventually, after a few hours, the transient peak at 369 nm starts to disappear. Meanwhile, the transient shoulder at 410 nm reaches its maximum of optical density after $t_a \simeq 30$ h and then decreases. Finally, after $t_a \simeq 300$ h, the spectra stop evolving. Note also the slight recovery of optical density of the original absorption band at 254 nm.

Fig. 5(b) summarizes the evolution of the optical density of the two transient bands at 369 nm and 410 nm, and of two wavelengths, 216 nm and 259 nm, close to the pyridine absorption at 254 nm. Note the similarity between the kinetics under UV radiation and after 15 min of radiation. The decrease of the absorption at 369 nm, and the transient shoulder at 410 nm, have a similar but much slower kinetics than under UV radiation. It suggests that the disappearance of the transient species responsible for the absorption band

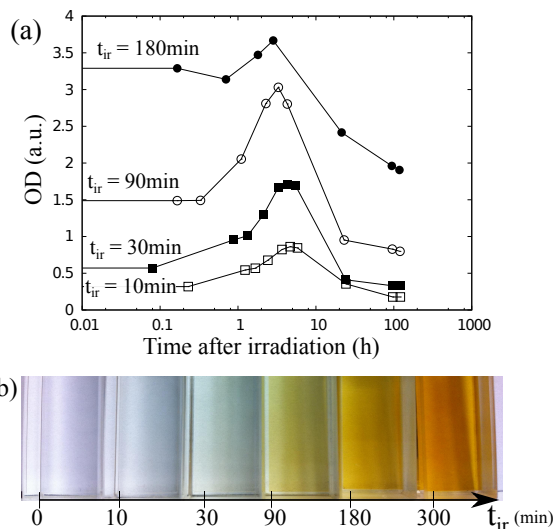


FIG. 6. (a) Photochemical kinetics for various irradiation durations and various times after irradiation. Evolution of the optical density maxima at 369 nm for irradiated concentrated solutions at 10 wt.% as a function of the time t_a after cessation of the irradiation. (b) Pictures of six 1 cm quartz cuvettes of concentrated CPCl at 10 wt.% irradiated using protocol 2. From left to right, $t_{ir} = 0, 10, 30, 90, 180, 300$ min. All the pictures were taken at the same time, a few week after irradiation ($t_a > 300$ h), showing the asymptotic coloration. The thickness of fluid along the line of sight is 2 mm.

at 369 nm and the shoulder at 410 nm is enhanced by UV radiation, but can also happen slower by thermal processes, and by action of generated free radicals, on time scales of the order of $t_{a0} = 100$ h.

3. Similar kinetics on more concentrated samples

To confirm that the new absorption band was indeed transient, even in the case of more concentrated samples, we performed kinetics on 10 wt.% CPCl solutions. Saturation prevented us from monitoring the disappearance of the CPCl absorption at 254 nm, but not the transient appearance of the absorption band at 369 nm. We irradiated four concentrated solutions for $t_{ir} = 10, 30, 90$ and 180 min, and then stored them in the dark at room temperature and monitored the evolution of the OD at 369 nm for various times t_a ranging from a few minutes to a week. The results are given on Fig 6(a). In a way similar to the 0.05 wt.% CPCl solutions, the measured optical densities for each duration of irradiation t_{ir} continues to evolve after the irradiation. The OD of the absorption band continues to increase, higher when the irradiation duration was long, then it decreases to reach a steady value, after a time t_{a0} of the order of 100 h, similar than in the dilute solution. We also noted a similar transient shoulder at 410 nm. For subsequent

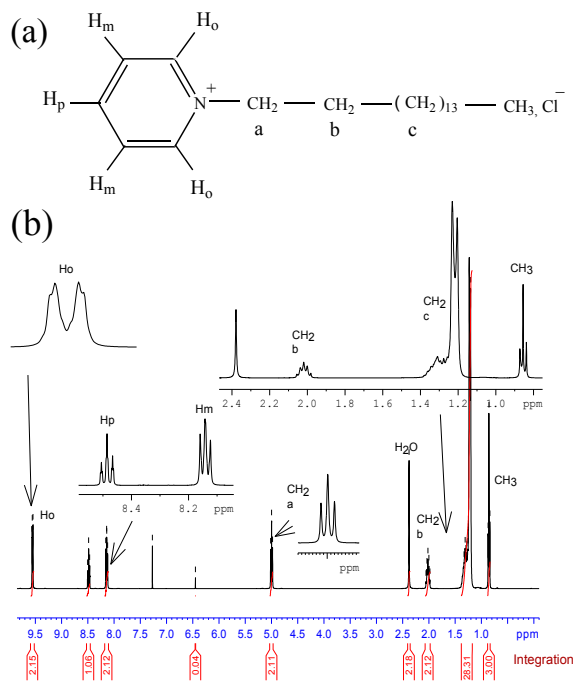


FIG. 7. (a) Structural formula of the CPCl molecule highlighting the different types of hydrogen atoms. (b) ^1H NMR in CDCl_3 of pure CPCl before irradiation.

times greater than t_{a0} , the spectra do not seem to evolve significantly, but are gradually shifted to an increasing wavelength with initial irradiation time t_{ir} .

Fig 6(b) shows pictures of quartz cuvettes of the 10 wt.% CPCl solutions for different irradiation times. The pictures show the gradient of colouring of the solutions, passing from transparent for the OS ($t_{ir} = 0$) to yellow and orange for $t_{ir} = 300\text{min}$. Those photographs were taken a few weeks after the irradiation ($t_a > t_{a0}$) so they show not only the gradient of color of the solutions according to the time of irradiation but also the final stability of this color. Samples obviously exhibit the shift in the absorption properties.

C. Characterization of the products using NMR spectroscopy

1. NMR spectrum of CPCl

The structure of the CPCl molecule is given in Fig. 7(a). For the original sample, each group of protons of the molecule was allotted to a peak of the NMR spectrum shown in Fig. 7(b). The chemical shifts δ (in ppm), the type of the peaks (singlets, doublets, triplets, quintuplets) and integrations are in complete agreement with the structure of the molecule. We have the aromatic H_o doublet at δ 9.54, the H_m triplet at δ 8.15, the H_p triplet at δ 8.48. In the aliphatic chain the first

CH_2 (a) gives a triplet at δ 4.99, the CH_2 (b) a quintuplet at δ 2, the CH_2 (c) a multiplet at δ 1.25, and finally, the CH_3 gives a triplet at δ 0.87. Note also the presence of H_2O at δ 2.6, coming from the mono-hydration of CPCl.

2. NMR spectra for various irradiation time

To better characterize the intermediate and final products of the photochemical reaction involving CPCl, we performed NMR spectroscopy of irradiated dilute samples after different irradiation durations. For those experiments, we used the same samples as for the UV-visible kinetics on Fig. 4, as described in the techniques section. Two representative spectra are given in Fig 8, for $t_{ir} = 15\text{min}$, allowing to show the transient products, and $t_{ir} = 4\text{h}$, to show the final products. We can observe the gradual disappearance of the aromatic bands, between 8 and 10 ppm, as well as the first CH_2 (a) triplet, near 5 ppm, right off the aromatic nucleus. There is a transient appearance of a series of doublets near 6 ppm, proof that the transient molecule still shows conjugations. After several hours of irradiation, the molecule becomes completely aliphatic, without any conjugation and does not show more than the CH_3 triplet and the CH_2 multiplet of the fatty chain. Note also that the H_2O at δ 2.6 on Fig. 7 coming from the mono-hydration of CPCl has disappeared.

III. DISCUSSION

We have showed that cetylpyridinium chloride solutions were indeed subjected to a photoreaction producing impurities. We have shown a photoreaction composed of two principal steps, and we have highlighted the differences in kinetics between dilute and concentrated solutions. Let us first compare the scenario and kinetics we observed in dilute solutions, with the known reactions concerning pyridine in aqueous solutions and polymers [9–11]. We will then discuss the specificities of the kinetics of the reaction in concentrated solutions.

First, from the results gathered on the dilute solutions, we can conclude that the cleavage of the pyridine ring of the cetylpyridinium chloride is essentially similar to the photohydration described succinctly by Andre *et al.* [10]. UV radiation around the absorption band of the pyridine, at 254nm cleaves a chemical bond, opens the aromatic ring and transforms it into an aldehyde enamine. On the UV-spectra, we observe the characteristic absorption band of the aldehyde enamine at 369nm [10], and the NMR spectra after $t_{ir} = 15\text{min}$ shows the appearance of a series of doublets near 6 ppm. In the case of pyridine, the aldehyde enamine is 5-amino-2,4-pentadienal. In the case of cetylpyridinium chloride, the aldehyde enamine has a long fatty chain off the NH_2^+ .

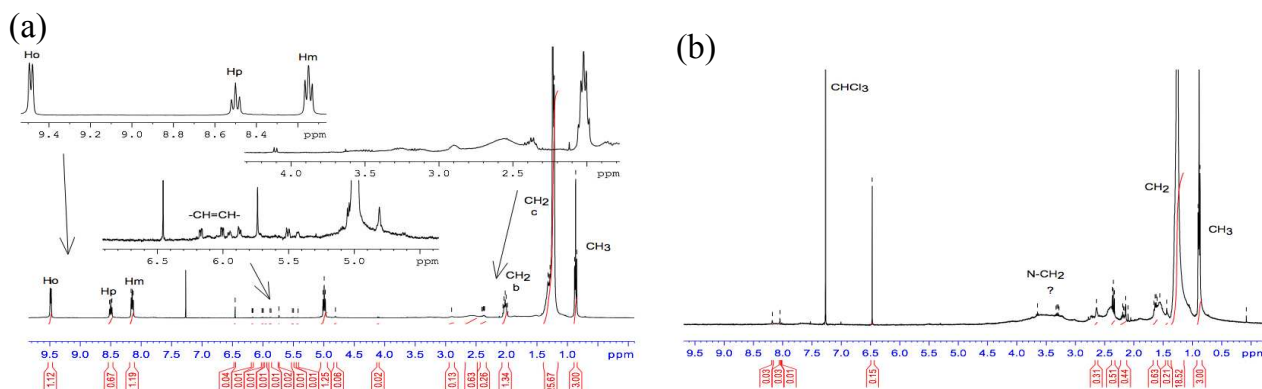
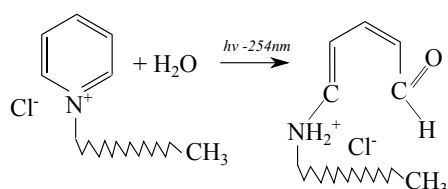


FIG. 8. (a) ^1H NMR in CDCl_3 of a dilute CPCI solution after $t_{ir} = 15\text{min}$, at the time when most of the CPCI has been transformed and the concentration of the transient species at 369nm is the highest. (b) ^1H NMR in CDCl_3 of a dilute CPCI solution after $t_{ir} = 4\text{h}$, when both the CPCI and the transient species at 369nm have disappeared, leaving the final product of the photoreaction.



The aldehyde enamine is unstable, and in the case of pure pyridine, the reaction is reversible if the solution is left in the dark at pH 8 [10]. But it had been noticed that the reaction can be irreversible if the aldehyde enamine can degrade into a third stable product, in particular, when the medium is acidic or basic [10], or when the aldehyde enamine interact with polymeric chains [11]. In our case, the reversibility seems indeed to be prevented by the fatty chain and/or the chloride ion. Note that the UV-visible spectra exhibits a shoulder at 410nm following the same kinetics than the transient band at 369nm. This shoulder is absent when pyridine is in aqueous solvent [10], but is characteristic of the presence of aldehyde enamine in a polymeric environment [11].

In our case, upon further irradiation, or by a slower thermally activated process, the aldehyde enamine was degraded into a third product. At long times, the band at 369nm disappears, and the NMR spectra changes from Fig 8(a) to Fig 8(b). Under UV irradiation, the degradation of the aldehyde enamine happens on time scales of the order of 100 min. Without UV irradiation, the degradation is much slower, on the order of a 100 h. The products of this degradation are more uncertain, but we can make a few hypothesis from the NMR spectra in Fig 8(b). The disappearance of the transient series of doublets near 6 ppm would suggest the disappearance of any conjugation. Finally, the increase of the relative integration of the CH_3 triplet at δ 0.87 between Fig 8(a) and Fig 8(b) would suggest that the connection between the ammonium and the fatty chain is broken, leaving free

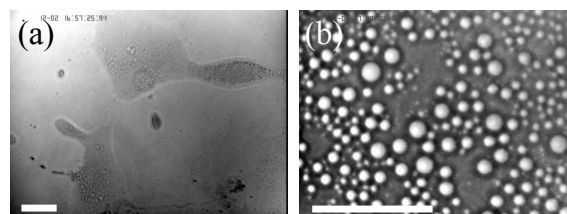


FIG. 9. Micrographs taken with an optical microscope with 10X (a) and 60X (b) objectives, showing the two phases structure of an irradiated concentrated CPCI sample with salts. The scale bar is $50\mu\text{m}$.

fatty chains of hexadecane as a third product.

Based on the unsaturated part of the UV-visible spectra on Fig. 3, and on the evolution of the OD on Fig. 6, it seems that the photochemical scenario in concentrated solutions is similar than in dilute solutions. In both cases, the aldehyde enamine is created by photohydration. The photohydration is irreversible in both cases, the fatty chain and/or the chloride ion being sufficient to prevent the reverse closure of the pyridine ring, as in polymeric environment [11]. None of the irradiated solutions in Fig. 6(b) recover their transparency, even after weeks being kept in the dark. Concerning the first step of the photochemical pathway, *i.e.* the opening of the pyridine ring, it seems that the only effect of the high concentration, is to limit the rate of the reaction. In a dilute solution, the maximum of absorption at 369 nm is reached only after 2 min, while in concentrated samples, the absorption is still growing after a few hours of irradiation. For pure pyridine in aqueous solution, it was reported that the rate of the photohydration of pyridine was essentially independent of the concentration [10]. Nonetheless, in our case, the increase of the concentration of CPCI also modifies the micellar structure from dilute spherical micelles to long entangled worms [1]. The modification

of the micellar structure could well change the rate of the photoreaction [12], such that even after a few hours of irradiation, only a minute fraction of the total mass of CPCl has been photohydrated.

Concerning the second step of the photochemical pathway, *i.e.* the breaking of the bond between the fatty chain and the head, it seems most likely that this process also occurs in concentrated solutions. Embedded into the bulk of the concentrated solution, the free fatty chains should then separate, because of their hydrophobic nature. Indeed, Fig. 9 shows micrographs of a thin layer of irradiated concentrated CPCl with salts, *i.e.* the solution used in rheological experiments, which show microdroplets organized in domains embedded in the original CPCl solution. The solution was irradiated for 30min, as described in section I. These droplets did not evolve with time and remained stuck on the surface of the cover slip. Further increase of the temperature from 25°C to

70°C did not produce any coalescence.

IV. CONCLUSION

In conclusion, our study shows that the photohydration of pyridine can occur when the pyridine ring forms the head of a surfactant. Since the micellar mesoscopic structure or the presence of chloride ions prevent the reversibility of the ring cleavage, temporary light exposure of cetylpyridinium chloride solutions, typically before rheological tests, can have additive effects. After several weeks, samples will acquire a slight yellow coloring evidencing the photochemical reactions. Such samples would contain impurities, mostly aldehyde enamine and hexadecane fatty chains. Some or all of those impurities can demix with the rest of the solution and can produce slip layers responsible for the abnormal shear-banding dynamics described in the article. We advise providers of CPCl and experimenters using CPCl to be particularly cautious with respect to light exposure of their samples.

-
- [1] J.F. Berret, Rheology of wormlike micelles : Equilibrium properties and shear-banding transition, Molecular gels, Elsevier (2005).
- [2] N. Müller, T. Wolff and G. von Büna, *J. Photochem.* **24**, 37 (1984).
- [3] T. Wolff *et al.*, *J. Phys. Chem.* **93**, 4894-4898 (1989).
- [4] A.M. Ketner *et al.*, *J. Am. Chem. Soc.* **129**, 1553-1559 (2007).
- [5] J.M.J. Paulusse and R.P. Sijbesma, *Angew. Chem., Int. Ed.* **45**, 2334-2337 (2006).
- [6] I. Tomatsu, A. Hashizume and A. Harada, *Macromolecules* **38**, 5223-5227 (2005).
- [7] P.J. Rankin, J.M. Ginder and D.J. Klingenberg, *Curr. Opin. Colloid Interface Sci.* **3**, 373 (1998).
- [8] J. Eastoe and A. Vesperinas, *Soft Matter* **1**, 338-347 (2005).
- [9] K.E. Wilzbach and D.J. Rausch, *J. Am. Chem. Soc.* **92**, 2178-2179 (1970).
- [10] J.C. Andre *et al.*, *J. Chem. Educ.* **54**, 387-388 (1977).
- [11] E. Vaganova *et al.*, *J. Fluorescence* **12**, 219-224 (2002).
- [12] N.J. Turro, G.S. Cox and M.A. Paczkowski, *Topics in Curr. Chem.* **129**, 57-97 (1985).
- [13] S. Lerouge and J.F. Berret, Shear-Induced Transitions and Instabilities in Surfactant Wormlike Micelles, *Adv. Polym. Sci.*, Springer Berlin/Heidelberg (2009).
- [14] M.P. Lettinga and S. Manneville, *Phys. Rev. Lett.* **103**, 248302 (2009).
- [15] K.W. Feindel and P.T. Callaghan, *Rheol. Acta* **49**, 1003-1013 (2010).
- [16] J.M. Adams, S.M. Fielding and P.D. Olmsted, *JNNFM* **151**, 101-118 (2008).
- [17] R. Buscall, *J. Rheol.* **546**, 1177-1183 (2010).